

## Proton diffusion in calcium hydroxide

This article has been downloaded from IOPscience. Please scroll down to see the full text article.

1990 J. Phys.: Condens. Matter 2 1499

(<http://iopscience.iop.org/0953-8984/2/6/009>)

View [the table of contents for this issue](#), or go to the [journal homepage](#) for more

Download details:

IP Address: 171.66.16.96

The article was downloaded on 10/05/2010 at 21:42

Please note that [terms and conditions apply](#).

## Proton diffusion in calcium hydroxide

S Mizrachi and M Hunger

Departamento de Física, Facultad de Ciencias, Universidad Central de Venezuela,  
Caracas 1041-A, AP 47726, Venezuela

Received 21 June 1988, in final form 18 August 1989

**Abstract.** A numerical method is presented for the calculation of the longitudinal relaxation time of proton diffusion in parallel hexagonal lattices of calcium hydroxide. A comparison between theoretical results and experimental data shows that the probability of a single proton jump is very high while the probability of two or more jumps can be almost neglected.

### 1. Introduction

A recent investigation of the magnetic relaxation of calcium hydroxide [1] showed evidence of at least two types of proton with different dynamics: localised precession and translational proton diffusion. The precession model has been confirmed by neutron diffraction experiments [2], infrared spectroscopy [3] and wide-band NMR data [4]. However, interpretation of proton conductivity measurements suggests that the presence of proton vacancies should be assumed [5, 6]. This assumption will be used to explain the temperature dependence of the translational proton diffusion which was attributed to the shorter of the two observed  $\text{Ca}(\text{OH})_2$  longitudinal relaxation times [1]. The lattice structure of calcium hydroxide has a  $D_{3d}^3$  ( $P\bar{3}m$ ) symmetry which generates a successive series of parallel layers with a  $-\text{Ca}-\text{O}-\text{H}-\text{H}-\text{O}-$  sequence. As the distance between neighbouring proton layers ( $0.64 \text{ \AA}$ ) is small compared with the distance between the next pair of layers, which is  $4.88 \text{ \AA}$ , we can assume that the proton motion is limited exclusively to the two bidimensional proton layers, stimulated by the presence of the proton vacancies mentioned above.

Torrey [7] proposed a random-walk diffusion model in three-dimensional crystals with symmetry inversion which allows calculation of the  $T_1$ ,  $T_2$  and  $T_{1\rho}$  relaxation times in the high-field approximation. This model has been applied for cubic crystals [8] but, unfortunately, cumbersome computations are required when it is used for calcium hydroxide as there is no symmetry inversion in the pair of proton layers. Therefore, in this paper a method is developed for the numerical calculation of the  $T_1$  relaxation time of a translational random-walk diffusion of the protons within two parallel planes of a hexagonal crystal structure. The model presented can be further developed to calculate the  $T_2$  and  $T_{1\rho}$  relaxation times. At the end of this paper the theoretical results are compared with experimental data.

## 2. Theory

The equation for the spin relaxation time  $T_1$ , in the high-field approximation, can be generally written as follows [9]:

$$1/T_1 = \frac{3}{2}\gamma^4\hbar^2 I(I+1)[J^{(1)}(\omega_0) + J^{(2)}(2\omega_0)] \quad (1)$$

where  $\gamma$  denotes the nuclear gyromagnetic constant,  $\omega_0 (= \gamma H_0)$  is the Larmor frequency associated with the strong external constant field  $H_0$  and  $I = \frac{1}{2}$  is the proton spin. The functions  $J^{(q)}(\omega)$ , with  $q = 1$  and  $2$ , are the spectral densities of the correlation functions  $G^{(q)}(t)$  and the diffusion process can be described by

$$J^{(q)}(\omega) = \int_{-\infty}^{\infty} G^{(q)}(t) \exp(i\omega t) dt \quad (2)$$

where

$$G^{(q)}(t) = \sum_{i,j} \langle F_{ij}^{(q)}(t') F_{ij}^{(q)}(t'+t) \rangle_{t'} \quad (3)$$

and

$$F_{ij}^{(q)}(t) = C_q Y_2^{(q)}(\theta_{ij}, \varphi_{ij}) / r_{ij}^3 \quad (4)$$

with

$$C_1^2 = 8\pi/15 \quad C_2^2 = 32\pi/15. \quad (5)$$

Here,  $\langle \rangle_{t'}$  symbolises the time average over all spin pairs  $i, j$  and  $(r_{ij}, \theta_{ij}, \varphi_{ij})$  are the spherical coordinates of the vector  $r_{ij}$  from spin  $i$  to spin  $j$  in the coordinate system where  $H_0$  is parallel to the  $z$  axis. The functions  $Y_2^{(q)}(\theta_{ij}, \varphi_{ij})$  are normalised second-order spherical harmonics.

In order to evaluate equation (1) the spectral density functions must be calculated. For that purpose the time average is replaced by an ensemble average [7]:

$$G^{(q)}(t) = \iint P(\mathbf{r}, \mathbf{r}_0, t) F_{ij}^{(q)}(\mathbf{r}_0) F_{ij}^{(q)*}(\mathbf{r}) f(\mathbf{r}_0) d\mathbf{r} \quad (6)$$

where  $P(\mathbf{r}, \mathbf{r}_0, t) d\mathbf{r}$  is the conditional probability that, if at zero time spin  $j$  is located at  $\mathbf{r}_0$  relative to spin  $i$ , at time  $t$  spin  $j$  will be inside the volume element  $d\mathbf{r}$  located at  $\mathbf{r}$  relative to the new position of spin  $i$ .  $N_0^{-1} f(\mathbf{r}_0) d\mathbf{r}$  is the probability that, at zero time, spin  $j$  is located within  $d\mathbf{r}_0$  at  $\mathbf{r}_0$  relative to spin  $i$ , where  $N_0$  designates the number of resonant nuclei. For a crystalline structure

$$f(\mathbf{r}_0) = \sum \delta(\mathbf{r}_0 - \mathbf{r}_k) \quad (7)$$

where the sum goes over all nuclei in the lattice. Substituting (7) into (6) we get

$$G^{(q)}(t) = \sum_{\mathbf{r}_k} F_{ij}^{(q)}(\mathbf{r}_k) \int P(\mathbf{r}, \mathbf{r}_k, t) F_{ij}^{(q)*}(\mathbf{r}) d\mathbf{r}. \quad (8)$$

The correlation function can be calculated by assuming that the proton moves through the lattice in the same way as a single proton would move through an otherwise empty lattice, jumping in a random walk to the first neighbours' sites. Let  $Q(\mathbf{r}, \mathbf{r}_k, t) d\mathbf{r}$  be the conditional probability that, if at  $t = 0$  a spin is located at  $\mathbf{r}_k$  with respect to the

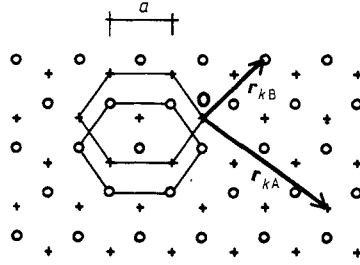


**Figure 1.** Vertical projection on the two planes A(+) and B(O) of the hexagonal lattices of Ca(OH)<sub>2</sub> which are separated by the vertical distance  $C_p$ .  $r_{kA}$  and  $r_{kB}$  are defined in the text.

origin, which is a lattice site, this spin moves to the position  $r$  at time  $t$ . Now,  $P(r, r_k, t)$  can be expressed as follows:

$$P(r, r_k, t) = \sum_{r_i r_j} Q(r_j, \mathbf{0}, t) Q(r_i - r_k, r_k, t) \delta[r - (r_i - r_j)] \quad (9)$$

where the sum goes over all lattice sites.

Equations (9) and (8) lead us to

$$G^{(q)}(t) = \sum_{r_k r_l r_j} Q(r_j, \mathbf{0}, t) Q(r_i - r_k, r_k, t) F_{ij}^{(q)}(r_k) F_{ij}^{(q)*}(r_i - r_j). \quad (10)$$

If  $R_n(r_l, r_k)$  denotes the probability that a spin in  $n$  jumps results in a change of the initial vector position from  $r_k$  to  $r_k + r_l$ , then

$$Q(r_l, r_k, t) = \sum_{n=0}^{\infty} R_n(r_l, r_k) w_n(t) \quad (11)$$

where  $w_n(t)$  is the probability that  $n$  jumps take place in the time interval  $(0, t)$ . For  $w_n(t)$ , it is usual to assume a Poisson distribution where  $\tau$  is the average waiting time of the proton at the lattice site:

$$w_n(t) = (1/n!) (t/\tau)^n \exp(-t/\tau). \quad (12)$$

Substituting (11) and (12) in (10) we get

$$G^{(q)}(t) = \exp(-2t/\tau) \sum_{\substack{r_k r_l r_j \\ n, n' = 0, \infty}} R_n(r_j, \mathbf{0}) R_{n'}(r_i - r_k, r_k) \frac{1}{n! n'!} \left(\frac{t}{\tau}\right)^{n+n'} \times F_{ij}^{(q)}(r_k) F_{ij}^{(q)*}(r_i - r_j). \quad (13)$$

Since we assume just single jumps to nearest-neighbour sites, then the proton will hop consecutively between the two plane hexagonal lattices (A and B) separated by the vertical distance  $C_p$  (figure 1). If  $r_{kA}$  represents the vector from the origin 0 to any point  $K$  in the hexagonal lattice A (where 0 is located), and  $r_{kB}$  is the vector from 0 to any point  $K$  in the lattice B, then the probabilities  $R_n(r_l, r_k)$  fulfil the following symmetry conditions:

$$R_n(r_l, r_{kA}) = R_n(r_l, \mathbf{0}) \quad (14a)$$

$$R_n(r_l, r_{kB}) = R_n(-r_l, \mathbf{0}). \quad (14b)$$

Using these equations in (13) and substituting the result into (2), the spectral density becomes

$$J^{(q)}(\omega) = \frac{1}{\omega} \sum_{\substack{\mathbf{r}, \mathbf{r}_j \\ n, n' = 0, \infty}} R_n(\mathbf{r}_j, \mathbf{0}) R_{n'}(\mathbf{r}_i, \mathbf{0}) \binom{n+n'}{n} \frac{1}{2^{n+n'}} j_{n+n'}(\omega\tau) \\ \times \left( \sum_{\mathbf{r}_{kA}} F_{ij}^{(q)}(\mathbf{r}_{kA}) F_{ij}^{(q)*}(\mathbf{r}_{kA} + \mathbf{r}_i - \mathbf{r}_j) \right. \\ \left. + \sum_{\mathbf{r}_{kB}} F_{ij}^{(q)}(\mathbf{r}_{kB}) F_{ij}^{(q)*}(\mathbf{r}_{kB} - \mathbf{r}_i - \mathbf{r}_j) \right) \quad (15)$$

with

$$j_s(\omega\tau) = \frac{\omega\tau}{[1 + (\omega\tau/2)^2]^{s+1}} \sum_{l=0}^u (-1)^l \binom{s+1}{2l} (\omega\tau/2)^{2l} \quad (16)$$

where  $u$  is the greatest integer  $\leq (S+1)/2$ .

In the appendix we show how equation (15) can be transformed to the more compact form:

$$J^{(q)}(\omega) = \frac{1}{\omega} \sum_{N(\text{even})} \left( \sum_{\mathbf{r}_{kA}, \mathbf{r}'_{kA}} F_{ij}^{(q)}(\mathbf{r}_{kA}) F_{ij}^{(q)*}(\mathbf{r}_{kA} + \mathbf{r}'_{kA}) R_N(\mathbf{r}'_{kA}, \mathbf{0}) \right. \\ \left. + \sum_{\mathbf{r}_{kB}, \mathbf{r}'_{kA}} F_{ij}^{(q)}(\mathbf{r}_{kB}) \frac{1}{2} [F_{ij}^{(q)*}(\mathbf{r}_{kB} - \mathbf{r}'_{kA}) \right. \\ \left. + F_{ij}^{(q)*}(\mathbf{r}_{kB} - \mathbf{r}'_{kA} - 2C_p \hat{n})] R_N(\mathbf{r}'_{kA}, \mathbf{0}) \right) j_N(\omega\tau) \\ + \frac{1}{\omega} \sum_{N(\text{odd})} \left( \sum_{\mathbf{r}, \mathbf{r}'_{kB}} F_{ij}^{(q)}(\mathbf{r}) F_{ij}^{(q)*}(\mathbf{r} - \mathbf{r}'_{kB}) R_N(\mathbf{r}'_{kB}, \mathbf{0}) \right) j_N(\omega\tau) \quad (17)$$

where  $N = 0, 1, 2, \dots$  and  $\hat{n}$  is a unit vector normal to the plane A pointing towards the plane B. Furthermore,  $\mathbf{r}_{kA}$  and  $\mathbf{r}'_{kA}$  run over all the sites of lattice A and likewise  $\mathbf{r}_{kB}$  and  $\mathbf{r}'_{kB}$  over all the sites of lattice B, while  $\mathbf{r}$  points to lattice A or B. In the last equation, all terms which cancel the arguments of  $F_{ij}^{(q)}$  have to be excluded since two protons cannot occupy simultaneously the same site. The probabilities  $R_N(\mathbf{r}, \mathbf{0})$  can be calculated recursively [10].

For polycrystalline samples expression (17) has to be averaged over all crystal orientations with respect to  $H_0$ :

$$\langle J^{(1)}(\omega) \rangle = \frac{4}{30\omega a^6} \sum_{N=0}^{\infty} D_N^0 j_N(\omega\tau) \quad (18)$$

with

$$D_N^0 = \frac{a^6}{2} \sum_{\mathbf{r}, \mathbf{r}_{kA}} \frac{1}{|\mathbf{r}|^3 |\mathbf{r} + \mathbf{r}_{kA}|^3} \left( 3 \frac{|\mathbf{r} \cdot (\mathbf{r} + \mathbf{r}_{kA})|^2}{|\mathbf{r}|^2 |\mathbf{r} + \mathbf{r}_{kA}|^2} - 1 \right) R_N(\mathbf{r}_{kA}, \mathbf{0}) \quad N = 0, 2, 4, 6, \dots \quad (19a)$$

and

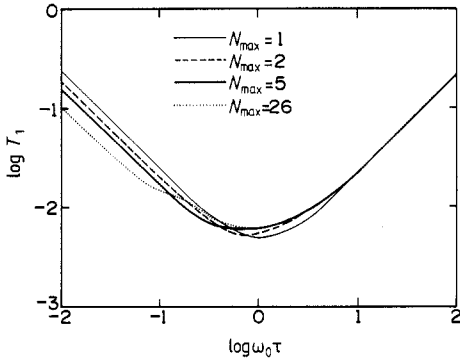


Figure 2. Double logarithmic plot of  $T_1$  against  $\omega_0\tau$  for  $\text{Ca}(\text{OH})_2$ , in units of  $5\omega_0 a^6 \gamma^{-4} \hbar^{-2} I^{-1} (I+1)^{-1}$ , calculated for  $N_{\max} = 1, 2, 5, 26$  with  $N_{\max}$  = upper limit of the  $N$  sum in equation (21).

$$D_N^0 = \frac{a^6}{2} \sum_{r_{kB}} \frac{1}{|r|^3 |r - r_{kB}|^3} \left( 3 \frac{|r \cdot (r - r_{kB})|^2}{|r|^2 |r - r_{kB}|^2} - 1 \right) R_N(r_{kB}, \mathbf{0}) \quad N = 1, 3, 5, \dots \tag{19b}$$

In addition

$$\langle J^{(2)}(\omega) \rangle = 4 \langle J^{(1)}(\omega) \rangle. \tag{20}$$

Substituting (19) and (20) into equation (1), we finally obtain:

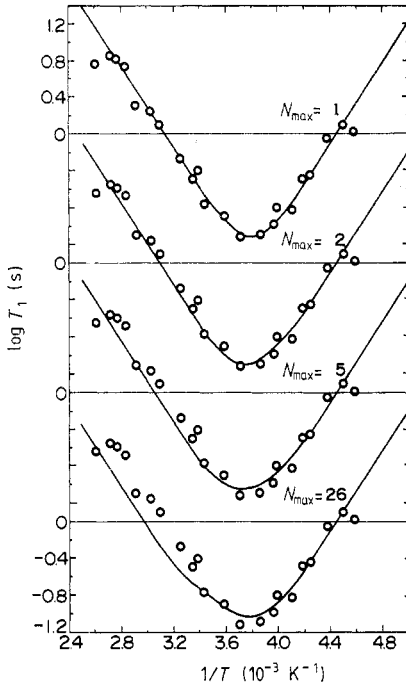
$$\frac{1}{T_1} = \frac{1}{5} \frac{\gamma^4 \hbar^2 I(I+1)}{\omega_0 a^6} \sum_{N=0}^{\infty} D_N^0 (j_N(\omega_0\tau) + 2j_N(2\omega_0\tau)). \tag{21}$$

Figure 2 illustrates the general behaviour of the longitudinal relaxation time for various  $N$  summations symbolised by  $N_{\max}$ , which always indicates the sum of integrals from 0 to  $N_{\max}$ . From the graph it is easy to see that the  $T_1$  curves coincide on the right-hand side of the minimum and differ considerably in shape on the left-hand side. This discrepancy increases with increasing  $N_{\max}$ , indicating width broadening of the  $T_1$  curve, displacement of the minimum and loss of the symmetry which separates the complete  $T_1$  curve into two regions.

### 3. Discussion

In a recent paper [1] concerning proton dynamics in  $\text{Ca}(\text{OH})_2$ , two longitudinal relaxations times of BPP-type were distinguished, in which the shorter one was attributed to a translational proton motion in bidimensional lattice layers. The measured relaxation time curve has a  $T_1$  minimum of about 7 ms at a temperature near 267 K and an activation energy of 0.44 eV. At a temperature close to 333 K the microdynamical mechanism defined by this relaxation time is dominant while at lower temperatures its influence decreases rapidly since it contributes little with 8% of the total relaxation below 285 K.

In the last section a formula was deduced for the longitudinal relaxation time of proton diffusion in a pair of bidimensional lattice layers (equation (21)). In order to compute the relaxation time using that equation we must evaluate the  $D_i^0$  ( $i = 1, 2, 3, \dots$ ) values. This was done using the lattice constants of  $\text{Ca}(\text{OH})_2$  at 260 K (at the  $T_1$  minimum) interpolated from experimental data [11]. Table 1 shows some of the



**Figure 3.** Temperature dependence of the measured values of the  $T_1$  relaxation time [1]. The full curves are the numerically calculated  $T_1$  curves for various numbers of proton jumps  $N_{\max}$ .

**Table 1.** List of  $D_i^0$  values for a lattice temperature of  $-13^\circ\text{C}$ .

|         |        |        |        |       |        |       |       |       |
|---------|--------|--------|--------|-------|--------|-------|-------|-------|
| $D_i^0$ | 69.284 | 12.825 | 20.732 | 6.739 | 11.016 | 4.837 | 7.354 | 3.908 |
| $i$     | 0      | 1      | 2      | 3     | 4      | 5     | 6     | 7     |
| $D_i^0$ | 5.795  | 3.336  | 4.748  | 2.932 | 4.015  | 2.628 | 3.543 | 2.389 |
| $i$     | 8      | 9      | 10     | 11    | 12     | 13    | 14    | 15    |

computed  $D_i^0$  data. The splitting in two different  $D^0$  sets ( $D_{2i}^0$  and  $D_{2i+1}^0$ ) is generated by the symmetry of the proton layers and cannot be observed in cubic lattices [7, 10, 12].

In order to compare the theoretical curve with the experimental results (shown in figure 3), we have assumed that the  $\tau$  against temperature relationship follows an Arrhenius law:

$$\tau = \tau_0 \exp(E/kT) \quad (22)$$

where  $T$  is the absolute temperature of the sample and  $E$  a thermal activation energy. The latter can be computed from the slopes of both wings of the  $T_1$  curve giving, of course, 0.44 eV as calculated before. Starting out from the fact that all curves must coincide in the low-temperature range, in accord with the experimental data, we obtain simultaneously a single value  $\tau_0 = 6.87 \times 10^{-18}$  s.

Since  $N_{\max} = 1$  gives the best fitting, we conclude that the probability of a single proton jump is the highest one and the likelihood of two or more jumps decreases when

the  $N_{\max}$  value is increased. This phenomenon is an interesting result and it could be explained by a continuous generation and recombination of proton vacancies as proposed by Freund and Wengeler [5]. This mechanism explains the electrical conductivity of  $\text{Mg}(\text{OH})_2$  which possesses the same atomic structure and electrical behaviour as  $\text{Ca}(\text{OH})_2$ , and it is obviously inhibiting an overwhelming number of proton jumps.

The proton vibration of 'umbrella' type [1], in this hydroxide, tends to average the dipolar interaction and therefore to increase the translational diffusion relaxation time  $T_1$ . As can be easily demonstrated in our case, this effect is not very significant since a precession angle close to  $5^\circ$  contributes less than 3% to the  $D_i^0$  values, which can be neglected. Furthermore, it is necessary to understand how a diffusion mechanism with a shorter longitudinal relaxation time than that of the umbrella precession does not dominate the magnetisation decay over the whole temperature range. The reason is that the vacancy concentration and the proton diffusion fall with decreasing temperature, whereas above 333 K the high number of vacancies makes the proton diffusion the dominant relaxation mechanism. This occurs exactly in the temperature range where the DC proton conductivity indicates a notable superionic behaviour [5].

Finally, the calculated activation energy of 0.44 eV is considerably lower than the reported value of 0.88 eV determined by proton conductivity measurements. However, such a discrepancy between NMR and conductivity data was reported and still remains an open question [13] which will be discussed in a forthcoming paper.

## Appendix

Equation (15) can be written

$$J^{(q)}(\omega) = \frac{1}{\omega} \sum_{r, r_{kA}} \sum_N S_{r,N}^- F_{ij}^{(q)}(r_{kA}) F_{ij}^{(q)*}(r_{kA} + r) + \frac{1}{\omega} \sum_{r, r_{kB}} \sum_N S_{r,N}^+ F_{ij}^{(q)}(r_{kB}) F_{ij}^{(q)*}(r_{kB} - r) \quad (\text{A1})$$

with

$$S_{r,N}^\pm = \sum_{\substack{n'+n=N \\ r_i \mp r_j = r}} R_n(r_i, \mathbf{0}) R_{n'}(r_j, \mathbf{0}) \binom{n'+n}{n} \frac{1}{2^{n'+n}}. \quad (\text{A2})$$

The theory of random flights yields for the probability  $R_n(\mathbf{r}, \mathbf{0})$ :

$$R_n(\mathbf{r}, \mathbf{0}) = \int_{r_1} \int_{r_2} \dots \int_{r_n} R_1(r_1, \mathbf{0}) R_1(r_2, \mathbf{0}) \dots \delta(r_1 - r_2 + r_3 \dots) dr_1 dr_2 \dots dr_n \quad (\text{A3})$$

where

$$R_1(r_1, \mathbf{0}) = \frac{1}{8\pi^3} \int_{\rho} A(\rho) \exp(-i\rho \cdot r) d\rho \quad (\text{A4})$$

and

$$A(\rho) = \frac{1}{3} (\exp(-i\rho \cdot r)\alpha + \exp(-i\rho \cdot r)\beta + \exp(-i\rho \cdot r)\gamma) \quad (\text{A5})$$



with  $\mathbf{r}$  ( $i = \alpha, \beta, \gamma$ ) denoting the vector from a lattice point A to the nearest-neighbour positions in lattice B. Substituting the delta function in (3) by its integral expression and taking into account (4) and (5), we get after integration of (3),

$$R_n(\mathbf{r}, \mathbf{0}) = \int_{\rho} A(\rho)A(-\rho) \dots \exp(-i\rho \cdot \mathbf{r}) d\rho \tag{A6}$$

which can be separated in

$$R_{2n}(\mathbf{r}, \mathbf{0}) = \int_{\rho} |A(\rho)|^{2n} \exp(-i\rho \cdot \mathbf{r}) d\rho \tag{A7a}$$

$$R_{2n+1}(\mathbf{r}, \mathbf{0}) = \int_{\rho} |A(\rho)|^{2n} A(\rho) \exp(-i\rho \cdot \mathbf{r}) d\rho \quad n = 0, 1, 2, 3, \dots \tag{A7b}$$

For the case  $\mathbf{r}_i - \mathbf{r}_j = \mathbf{r}$ :

$$\begin{aligned} S_{r,N}^- &= \frac{1}{2^N} \sum_{n'=0}^N \binom{N}{n'} \int_{r_i} \int_{r_j} R_{N-n'}(\mathbf{r}_j, \mathbf{0}) R_{n'}(\mathbf{r}_i, \mathbf{0}) \delta(\mathbf{r}_i - \mathbf{r}_j - \mathbf{r}) d\mathbf{r}_i d\mathbf{r}_j \\ &= \frac{1}{2^N} \sum_{n'=0}^N \binom{N}{n'} \frac{1}{8\pi^3} \int_{r_i} \int_{r_j} \int_{\rho} R_{N-n'}(\mathbf{r}_j, \mathbf{0}) R_{n'}(\mathbf{r}_i, \mathbf{0}) \\ &\quad \times \exp[i\rho \cdot (\mathbf{r}_i - \mathbf{r}_j - \mathbf{r})] d\mathbf{r}_i d\mathbf{r}_j d\rho. \end{aligned} \tag{A8}$$

If  $N$  is an odd number, and using (7), we get after integration

$$\begin{aligned} S_{r,N}^- &= \frac{1}{2^N} \sum_{n'(\text{even})}^N \binom{N}{n'} \frac{1}{8\pi^3} \int_{\rho} |A(\rho)|^{N-1} A(-\rho) \exp(-i\rho \cdot \mathbf{r}) d\rho \\ &\quad + \frac{1}{2^N} \sum_{n'(\text{odd})}^N \binom{N}{n'} \frac{1}{8\pi^3} \int_{\rho} |A(\rho)|^{N-1} A(\rho) \exp(-i\rho \cdot \mathbf{r}) d\rho \end{aligned} \tag{A9}$$

which can be rewritten as

$$S_{r,N}^- = \frac{1}{2}R(-\mathbf{r}, \mathbf{0}) + \frac{1}{2}R(\mathbf{r}, \mathbf{0}) \quad (N \text{ odd}). \tag{A10}$$

The above equation is zero except for  $\mathbf{r} = \pm \mathbf{r}_{kB}$ .

If  $N$  is even, it is easy to demonstrate that

$$S_{r,N}^- = R_N(\mathbf{r}, \mathbf{0}) \quad (N \text{ even}) \tag{A11}$$

which is zero except for  $\mathbf{r} = \mathbf{r}_{kA}$ . In the same way we get for odd  $N$ :

$$S_{r,N} = R_N(\mathbf{r}, \mathbf{0}) \quad (N \text{ odd}) \tag{A12}$$

which cancels to zero except for  $\mathbf{r} = \mathbf{r}_{kB}$ .

Finally,  $S_{r,N}^+$  can be written for even  $N$  as:

$$S_{r,N}^+ = \frac{1}{2^N} \sum_{n'(\text{even})}^N \frac{1}{8\pi^3} \binom{N}{n'} \int_{\rho} |A(\rho)|^N \exp(-i\rho \cdot r) d\rho \\ + \frac{1}{2^N} \sum_{n'(\text{odd})}^{N-1} \frac{1}{8\pi^3} \binom{N}{n'} \int_{\rho} |A(\rho)|^{N-2} A(\rho) A(\rho) \exp(-i\rho \cdot r) d\rho \quad (\text{A13})$$

which gives with (7):

$$S_{r,N}^+ = \frac{1}{2} R_N(r, 0) + \frac{1}{6} (R_{N-1}(r - r_{\alpha}, 0) + R_{N-1}(r - r_{\beta}, 0) + R_{N-1}(r - r_{\gamma}, 0)). \quad (\text{A14})$$

The values of  $r$  which do not make the last equation zero are  $r_{kA}$  and  $r_{kA} + 2C_p \hat{n}$ , where  $\hat{n}$  is a unit vector which is normal to the plane A and points towards the plane B. The sum in the parentheses is just equal to three times the probability that a spin leaving the origin arrives after  $N$  steps to a site in the lattice B with the nearest neighbours  $r - r_i$  ( $i = \alpha, \beta, \gamma$ ), which means:

$$S_{r,N}^+ = \frac{1}{2} R_N(r, 0) + \frac{1}{2} R_N(r - 2C_p \hat{n}, 0) \quad (N \text{ even}). \quad (\text{A15})$$

Substituting (10), (11), (12) and (15) into (1) shows that equation (17) of § 2 can be easily verified.

## References

- [1] Moreno J A, Mizrahi S and Oppeltz V 1984 *Solid State Commun.* **51** 597
- [2] Busing W R and Levy H A 1957 *J. Chem. Phys.* **48** 2032
- [3] Busing W R and Morgan H W 1958 *J. Chem. Phys.* **28** 998
- [4] Holuj F and Wieczorek J 1976 *Can. J. Phys.* **55** 654
- [5] Freund F and Wengeler H 1980 *Ber. Bunsenges. Phys. Chem.* **84** 866
- [6] Freund F, Wengeler H and Martens R 1980 *J. Chem. Phys.* **77** 837
- [7] Torrey H C 1953 *Phys. Rev.* **92** 962
- [8] Wolf D 1975 *J. Magn. Res.* **17** 1
- [9] Abragam A 1962 *The Principles of Nuclear Magnetism* (Oxford: Clarendon) Ch. VIII
- [10] Pasemann L and Schneider H 1973 *J. Magn. Res.* **9** 255
- [11] Petch H E 1961 *Acta Crystallogr.* **14** 950
- [12] Sholl C A 1974 *J. Phys. C: Solid State Phys.* **7** 3378
- [13] Arribart H and Piffart Y 1983 *Solid State Commun.* **45** 571